

DFT Analysis of Cubane-Type $FeIr_3S_4$ Clusters. Dinitrogen Binding and Activation at the Tetrahedral Fe Site

Pawel M. Kozlowski,*[1,3] Yoshihito Shiota,[1] Satomi Gomita,[2] Hidetake Seino,[2] Yasushi Mizobe,*[2] and Kazunari Yoshizawa*[1]

[1]Institute for Materials Chemistry and Engineering, Kyushu University, Motooka, Nishi-ku, Fukuoka 819-0395

[2]Institute of Industrial Science, The University of Tokyo, Komaba, Meguro-ku, Tokyo 153-8505

[3]On sabbatical leave from Department of Chemistry, University of Louisville, Louisville, Kentucky 40292, USA

Received May 21, 2007; E-mail: kazunari@ms.ifoc.kyushu-u.ac.jp

The electronic and structural properties of the cubane-type mixed-metal sulfido clusters with a $FeIr_3S_4$ core and possible dinitrogen binding and activation were analyzed by density functional theory (DFT) calculations. Five different charges of the cluster and manifold of the electronic states were investigated. For each charge under consideration $(+2, +1, 0, -1, -2)$ systematic analysis of structural and electronic properties was carried out. The DFT calculations show that both Fe–N and N≡N bond lengths correlate with the total charge of the cluster. The length of the Fe–N bond decreased, whereas the N≡N bond length increased with the number of added electrons. However, only noticeable elongation of the N≡N bond was observed when the charge of the cluster became negative. Similar analysis was extended to species that have protonated dinitrogen bond. The results obtained from the DFT analysis are useful in considering the principles of the reduction of dinitrogen to ammonia at a single metal center.

Natural enzyme nitrogenase can catalyze the conversion of molecular nitrogen into ammonia through coupled protonation and electronation.[1] Given the extremely drastic conditions required for the industrial ammonia synthesis from N_2 and H_2 gases with the Fe-based Haber–Bosch catalyst,[2] it is quite noteworthy that biological N_2 fixation proceeds under ambient conditions, that is, atmospheric pressure and room temperature. Clarification of the details of this remarkable N_2-fixing enzyme is therefore the subject of extensive studies to aid in the development of new commercial N_2-fixing systems that can operate under milder conditions than those for the present processes.

Recent X-ray diffraction studies on the Mo-dependent nitrogenase have disclosed the structure of the active site of this enzyme called FeMo cofactor to be a complicated mixed-metal sulfido cluster formulated as $MoFe_7S_9X$ (Fig. 1),[3] where X is most probably N.[4] It should be noted that this X-ray structure corresponds to that of the resting state of the enzyme and donation of multiple electrons and protons to this site is necessary prior to the binding and reduction of nitrogenase substrates, such as N_2 and acetylene.

Despite the significant progress in the elucidation of the active site structure of nitrogenase, no direct information has yet been available concerning where and how N_2 binds to FeMo cofactor, and it is quite difficult to obtain such information experimentally from enzymes. Synthetic model approach is therefore quite promising to shed light on this problem.[5]

It is now well known that N_2 can bind to transition metal centers to give various stable N_2 complexes and, interestingly, the studies on the reactivities of some selected Mo dinitrogen complexes with *P*- and *N*-donor coligands have afforded important information on the protonation mechanism of N_2 coordinated to the Mo center.[6] However, the Mo dinitrogen complexes with sulfido ligands are yet unknown. On the other hand, there is some recent experimental and theoretical findings, which suggests that N_2 binds to the Fe atom(s) in FeMo cofactor.[7] However, there is no precedence for the coordination of N_2 to the Fe center with sulfido ligands,[8] and Fe N_2 complexes that are amenable to protonation at the N_2 ligand in a well-defined manner are still scarce.[9]

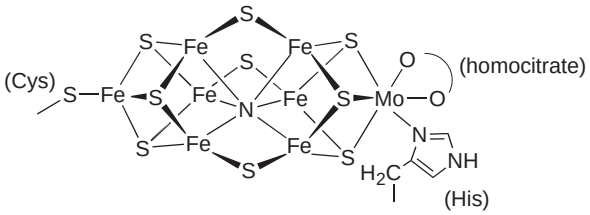

Fig. 1. Structure of FeMo cofactor.

In this context, we have started the DFT studies on the metal sulfido clusters prepared as the model of FeMo cofactor,[10] whereby our attention has focused on the Mo and Fe centers embedded in the cubane cores as observed in the nitrogenase active site. Thus, the previous paper dealt with the octahedral Mo site in the cubane-type cluster $[(CpRu)_2\{MoCl_2(MeCN)\}_2(\mu_3\text{-}S)_4]$ $(Cp = \eta^5\text{-}C_5H_5)$, of which the structure was modeled based on the X-ray structure of the Cp* analogue $[(Cp^*Ru)_2\{MoCl_2(MeCN)\}_2(\mu_3\text{-}S)_4]$ $(Cp^* = \eta^5\text{-}C_5Me_5)$. This study has shown that in contrast to the considerable stable binding of MeCN to this Mo site, isoelectronic N_2 molecule hardly coordinates to the Mo centers in a stable manner. However, it has been suggested that donation of two electrons to this cluster core can strengthen the Mo–N bond of the Mo–N≡N moiety significantly.[11] Now, we carried out the present DFT study

Published on the web December 13, 2007; doi:10.1246/bcsj.80.2323

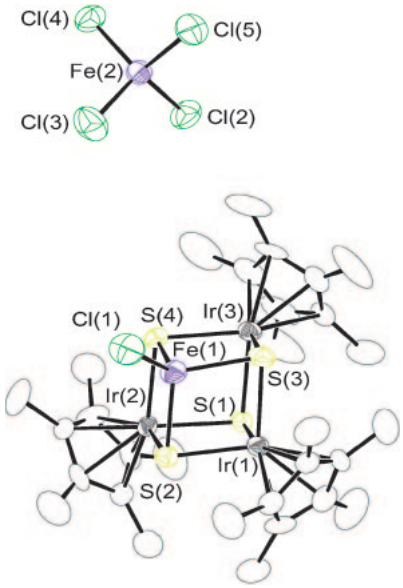

Fig. 2. X-ray structure of $[(Cp^*Ir)_3(FeCl)(\mu_3\text{-}S)_4][FeCl_4]$ (**1**). Hydrogen atoms and solvating THF molecules are omitted for clarity.

on the cubane-type $FeIr_3S_4$ cluster containing a tetrahedral Fe site surrounded by three μ-sulfido ligands on the basis of the X-ray structure of $[(Cp^*Ir)_3(FeCl)(\mu_3\text{-}S)_4][FeCl_4]$ (**1**) and estimated the N_2-binding ability of the vacant site of the Fe site generated after dissociation of the Cl anion. Stability and bonding feature of the diazenido NNH ligands on this Fe site were also calculated.

Experimental

X-ray Crystallography for 1. Single crystals of **1**·1.5THF (Fig. 2) were obtained as the minor product in quite low yield from the reaction of $[(Cp^*Ir)_3(\mu\text{-}S)(\mu\text{-}SH)_3]Cl$ (57 mg, 0.050 mmol) with $FeCl_3$ (8 mg, 0.05 mmol) in the presence of 4 equiv of NEt_3 in MeCN (5 mL) at 0 °C and subsequent crystallization of the product mixture using THF as a solvent. Characterization of the major product has been yet unsuccessful.

A crystal suitable for the X-ray diffraction study was sealed in a glass capillary under argon and mounted on a Rigaku Mercury-CCD diffractometer equipped with a graphite-monochromatized Mo Kα Source. All diffraction studies were done at 23 °C.

Structure solution and refinements were carried out by using the Crystal Structure program package.[12] The positions of the non-hydrogen atoms were determined by Patterson methods (PATTY)[13] and subsequent Fourier synthesis (DIRDIF 99).[14] These were refined with anisotropic thermal parameters by full-matrix least-squares techniques. Hydrogen atoms were placed at the calculated positions and included in the final stages of refinements with fixed parameters. Selected crystallographic data for **1**·1.5THF are as follows: $C_{36}H_{57}Cl_5Fe_2Ir_3O_{1.5}S_4$, fw: 1507.70, triclinic, space group $P\bar{1}$ (No. 2), $a = 13.354(3)$, $b = 13.600(3)$, $c = 16.869(4)$ Å, $\alpha = 66.50(1)$, $\beta = 68.04(1)$, $\gamma = 65.55(1)°$, $V = 2476.5(9)$ Å^3, $Z = 2$, μ(Mo Kα) = 90.91 cm^{-1}, $\rho_{calcd} = 2.022$ g cm^{-3}, crystal size $0.25 \times 0.20 \times 0.10$ mm^3, $R1 = 0.054$ for 4443 data with $I > 2\sigma(I)$ and $wR2 = 0.178$ for total 10901 unique reflections and 449 variables (GOF = 1.019). Selected interatomic distances and angles are listed in Table 1. The crystal data have been deposited at CCDC, Cambridge, UK and given the reference number CCDC 659187. Copies of the data can be obtained free of charge via http://www.ccdc.cam.ac.uk/conts/retrieving.html (or from the Cambridge Crystallographic Data Centre, 12, Union Road, Cambridge, CB2 1EZ, UK; Fax: +44 1223 336033; e-mail: deposit@ccdc.cam.ac.uk).

Table 1. Selected Interatomic Distances and Angles in **1**

(a) Distances/Å			
Ir(1)···Ir(2)	3.579(1)	Ir(1)···Ir(3)	3.614(1)
Ir(1)···Fe(1)	2.897(2)	Ir(2)···Ir(3)	3.5997(8)
Ir(2)···Fe(1)	2.936(3)	Ir(3)···Fe(1)	3.162(3)
Ir(1)–S(1)	2.383(6)	Ir(1)–S(2)	2.325(4)
Ir(1)–S(3)	2.365(4)	Ir(2)–S(1)	2.391(3)
Ir(2)–S(2)	2.318(6)	Ir(2)–S(4)	2.364(4)
Ir(3)–S(1)	2.400(3)	Ir(3)–S(3)	2.376(6)
Ir(3)–S(4)	2.377(4)	Fe(1)–Cl(1)	2.163(6)
Fe(1)–S(2)	2.257(4)	Fe(1)–S(3)	2.273(4)
Fe(1)–S(4)	2.305(7)		
(b) Angles/°			
Cl(1)–Fe(1)–S(2)	110.7(2)	Cl(1)–Fe(1)–S(3)	119.2(3)
Cl(1)–Fe(1)–S(4)	120.5(3)	S(2)–Fe(1)–S(3)	104.6(2)
S(2)–Fe(1)–S(4)	102.9(2)	S(3)–Fe(1)–S(4)	96.6(2)

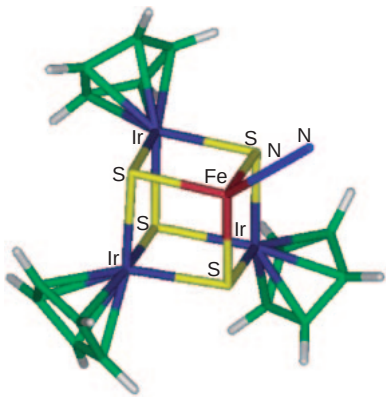

Fig. 3. Structural model of $[(CpIr)_3(FeN_2)(\mu_3\text{-}S)_4]^{2+}$ cluster used in DFT analysis.

Method of Calculation. All the calculations reported in this work were carried out using non-local DFT with the hybrid Becke–Lee–Yang–Parr (B3LYP) functional[15,16] and the LACVP+* basis set as implemented in the Jaguar[17] suite of programs for electronic structure calculations. This level of theory was found appropriate for structural analysis and electronic properties of $Mo_2Ru_2S_4$ metal clusters employed in previous DFT analysis.[11] The crystallographic coordinates of parent compound **1** were used to build a computational model of $FeIr_3S_4$ cluster in which Cp* (Cp* = η^5-C_5Me_5) was simplified by Cp (Cp = η^5-C_5H_5), as shown in Fig. 3.

The formal charges of the Cp rings and the chlorine atom are −1, and that of the sulfur atoms are −2. The formal charge of the Ir ions in this complex was counted to be +3, and therefore, they have a closed-shell d^6 configuration, whereas that of the Fe ion was counted to be +4, thus having a d^4 electronic configuration. Thus, the total charge of the $FeIr_3S_4$ cluster in Fig. 2 is +1, but when the Cl atom was replaced by N_2 in DFT analysis, the total charge becomes +2 in Fig. 3. To evaluate the accuracy of the DFT calculations, we compared the computational model in

Fig. 3 and the X-ray structure of $[(Cp^*Ir)_3(FeCl)(\mu_3\text{-}S)_4][FeCl_4]$ in Table 1. The Fe–S, Ir–S, Fe–Ir, and Ir–Ir distances in the optimized structure of the ground quintet state are on average 2.348, 2.367, 3.021, and 3.650 Å, respectively, whereas the Fe–S, Ir–S, Fe–Ir, and Ir–Ir distances in the X-ray structure are 2.278, 2.366, 2.998, and 3.600 Å, respectively. Thus, the DFT calculations are fully consistent with the X-ray structure with respect to the cubane-type metal–sulfur framework. Noodleman and co-workers[18] have demonstrated that iron-containing cubane-type clusters have a dense manifold of electronic states arising from different spin couplings and that some of them can be characterized via DFT calculations. These electronic states in DFT calculations can be controlled by total charge (q) and spin multiplicity (M_s). In the case of $[(CpIr)_3(FeN_2)(\mu_3\text{-}S)_4]^q$, they are denoted as (q, M_s) throughout this paper.

Results and Discussion

Binding of N_2 at the Fe Site. The focal point in efficient nitrogen fixation is the cleavage of the nitrogen–nitrogen triple bond with a dissociation energy of 225 kcal mol^{-1} under mild conditions. The key to the reductive activation of the triple bond is how to fill the degenerate π_g^* orbitals or the high-lying σ_g^* orbital of dinitrogen. The first step to understand this issue is the interaction between the dinitrogen and $FeIr_3S_4$ cluster at the coordinatively unsaturated Fe site. In order to estimate this interaction, we computed energy curves between dinitrogen and cluster as a function of the Fe–N distance, as shown in Fig. 4. The interaction curve, which represents the lowest electronic state denoted as (+2, 5), has a minimum at ≈2.2 Å and binding energy of about −11.1 kcal mol^{-1}. This binding energy may be partially overestimated, due to the involvement of charged species. In order to obtain more reliable estimate, we compared similar energy curves for two other electronic states, where the $FeIr_3S_4$ cluster has a total charge equal to +1 and 0 (Fig. 4). The binding energy diminishes with an increase in the total charge; in the case of the sextet state with a total charge equal to +1, it was −5.5 kcal mol^{-1}, whereas for the neutral quintet state, it was found to be about −2.5 kcal mol^{-1}. In general, the interaction between dinitrogen and the $FeIr_3S_4$ cluster is weak, indicating that the triple bond of N_2 cannot be activated effectively under such conditions. The increase in the total charge makes the interaction weaker and, at the same time, has essentially no influence on the iron–nitrogen distance, as seen in Fig. 4. This finding is fully consistent with previous analysis reported for the $Mo_2Ru_2S_4$ cluster, where the interaction energy was found to be about 5 kcal mol^{-1}.[10] In contrast to the previous DFT analysis, however, the optimized Fe–N_2 distance is shorter, approximately equal to 2.2 Å, in comparison to the longer Mo–N_2 distances of 2.7 or 2.4 Å found for the $Mo_2Ru_2S_4$ clusters. This metal–N_2 bond shortening may indicate that the binding of dinitrogen to the coordinatively unsaturated Fe atom with the oxidation states from +2 to 0 is more effective than that to the Mo^V and Mo^{IV} centers for nitrogen–nitrogen bond activation.

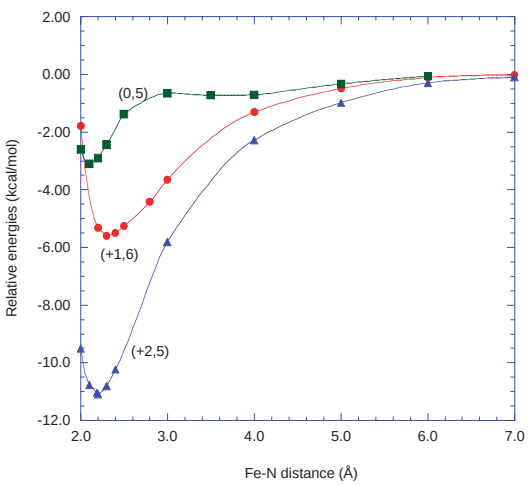

Fig. 4. Interaction energy curves of the (+2, 5), (+1, 6), and (0, 5) states computed at the B3LYP/LACVP+* level of theory. Total charge (q) and multiplicity (M_s) are denoted as (q, M_s).

N_2 Activation by $FeIr_3S_4$ Cluster. Many efforts have been undertaken over the past few years to build low-molecular-weight transition-metal complexes that can mimic structural or functional models of nitrogenase. It has been demonstrated that cubane-type clusters that are chemically and structurally related to FeMo cofactor (Fig. 1) exhibit only limited reactivity with respect to N_2 fixation.[19] On the other hand, the principles of reduction of nitrogen to ammonia at a single metal center (M = Mo or W) have been extensively studied since pioneering work by Chatt et al. and Hidai et al.,[5,6] and more recently by Schrock.[21] It has demonstrated that dinitrogen can bind to a single metal center and reduced to ammonia through a series of intermediates containing M–N≡N, M–N=NH, M=N–NH_2, M≡N, M=NH, M–NH_2, and M–(NH_3) moieties.[5,6,20]

Correlation between (q, M_s) Electronic States and Fe–N≡N Bond Lengths. The activation of N≡N by the $FeIr_3S_4$ cluster can be discussed in the context of cubane-type cluster as well as single metal center, due to the closed-shell character of the iridium atoms. In a recent review, Studt and Tuczek[21] have divided dinitrogen complexes into weakly, moderately, and strongly activated systems depending on N–N distances and stretching frequencies. As discussed above, the $[(CpIr)_3(FeN_2)(\mu_3\text{-}S)_4]^q$ models with $q = +2$, +1, or 0 fall into weak activation category, whereas the reactivity leading to generation of NH_3 from N_2 requires at least moderately activated compounds.[21] Therefore, does modification of electronic structure changes their ability with respect to N_2 activation? More specifically, how electronic structure of the $FeIr_3S_4$ cluster (Fig. 3) should be modified in order to observe noticeable changes of the Fe–N≡N bond lengths required for moderately activated systems. To accomplish this, five different charges of the cluster and manifold of the electronic states were investigated. For each charge under consideration, $q = +2$, +1, 0, −1, or −2, the structure of the cluster was fully optimized assuming different spin states. Calculated energies in the (q, M_s) electronic states are listed in Table 2. For each optimized structure, systematic structural analysis was carried out. The most important bond lengths associated with the Fe–N≡N unit are plotted in Fig. 5.

The DFT optimized bond lengths show that both N≡N and Fe–N distances correlate with the total charge of the cluster. The length of the Fe–N bond decreased whereas the N≡N bond length increased with the number of added electrons. There are not much changes observed for charges equal to

Table 2. Calculated Energies (in the Unit of Hartree) of the $FeIr_3S_4$ Clusters in the (q, M_s) Electronic States

	+2	+1	0	−1	−2
Sextet		−2720.5280837		−2720.7498614	
Quintet	−2720.191839		−2720.7295443		−2720.6974138
Quartet		−2720.5242075		−2720.7859679	
Triplet	−2720.1877894		−2720.7094725		−2720.6952953
Doublet		−2720.505778		−2720.7491797	

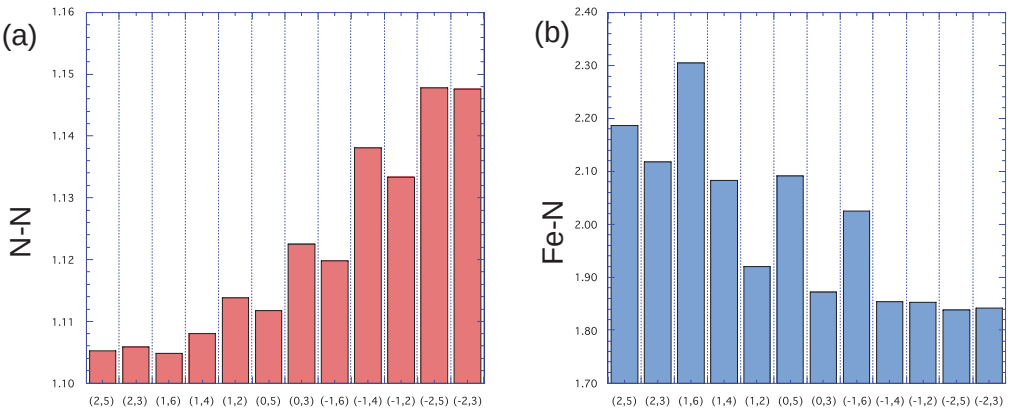

Fig. 5. Optimized N–N and Fe–N bond lengths corresponding to different electronic states (q, M_s) of $[(CpIr)_3(FeN_2)(\mu_3\text{-}S)_4]^{+q}$ computed at the B3LYP/LACVP+* level of theory.

+2 or +1, respectively. The first change was observed when the charge of the cluster was equal to zero. On the other hand, noticeable elongation of the N≡N bond was observed when the charge of the cluster became negative. By increasing the number of added electrons, the dinitrogen bond can be effectively activated.

The results of the DFT analysis can be supported by analysis in terms of cluster frontier MOs. For this purpose, we extracted MOs located near HOMO/LUMO gap from the neutral complex, as shown in Fig. 6. These MOs provide further insight into the subject of N–N bond activation. As can be seen from their contours, all occupied MOs (i.e. HOMO, HOMO−1, ..., HOMO−4) have dominant cubane-type character. They mostly involve iron, iridium, and sulfur with no contribution from the nitrogen orbitals. On the other hand, LUMO and LUMO+1 are essentially pure π_g* MOs of the coordinated N_2. As has been pointed out before, the key step to achieve the reductive activation of the triple bond is to fill the degenerate π_g* orbitals of dinitrogen. Thus, addition of one or two electrons fulfills this condition and generates longer N–N bond as a consequence of their occupancy.

Correlation between (q, M_s) Electronic States and Fe–N=N–H Bond Lengths. The conversion of N_2 to ammonia by mono-transition-metal complexes involves a sequence of protonation and reduction steps.[20] The reduction mechanism has been investigated experimentally and supported by DFT calculations.[21,22] In order to further understand the properties of the $FeIr_3S_4$ cluster, the terminal nitrogen has been protonated and different combinations of charges and spin states investigated. Based on previous analysis, we focused our attention on complexes which have an overall neutral or negative charge. A total of seven different electronic states were investigated, as summarized in Fig. 7.

For each particular combination of charge and spin multiplicity, the structure was optimized and relevant distances extracted from calculations. The trend observed for nitrogen–nitrogen bond lengths is consistent with the previous analysis. The increase in the number of added electrons is associated with elongation of the bond length in the range from ca. 1.19 to 1.25 Å. For comparison, a typical N–N double bond distance is ca. 1.25 Å as observed for RN=NR (R = aryl). The trend was opposite for Fe–N where a decrease in distance between iron and nitrogen was observed. In addition the Fe–N bond lengths depended on spin multiplicity, that is, the higher multiplicity the longer distance. At the same time, different spin multiplicities had only minor influence on the nitrogen–nitrogen distance.

Summary and Conclusion

The catalytic conversion of nitrogen to ammonia is not only important from technological point of view but also is one of the key reactions in biology. Biological N_2 fixation involves FeMo cofactor of which the catalytic function remains poorly understood. In particular, it is not known how N_2 binds to FeMo cluster and precisely how ammonia is generated by a sequence of protonation and reduction steps. In order to elucidate this fundamental issue, cubane-type mixed-metal sulfido clusters with a $FeIr_3S_4$ framework were synthesized and structurally characterized by using X-ray crystallography. To estimate the N_2-binding ability of the vacant site of the Fe site, the Cl anion was replaced by –N≡N, and density functional theory was applied to analyze the structural and electronic properties of the cluster. We showed that dinitrogen bond length correlates with the total charge of the cluster although

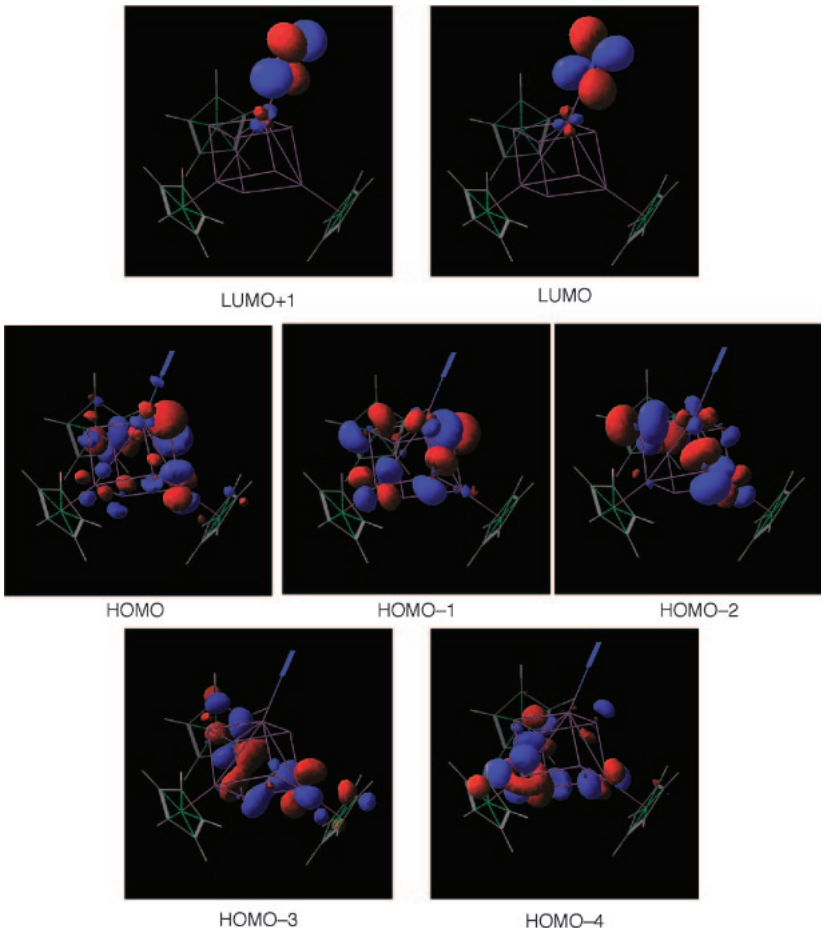

Fig. 6. Frontier molecular orbitals associated with $[(CpIr)_3(FeN_2)(\mu_3\text{-}S)_4]^0$.

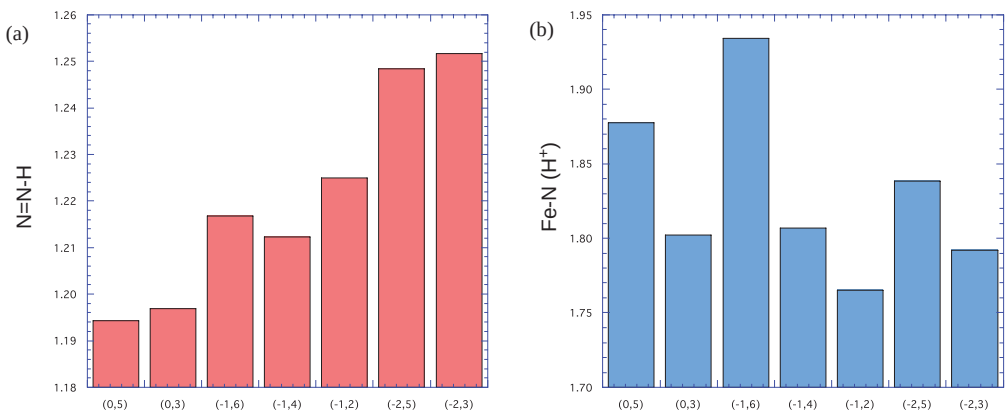

Fig. 7. Optimized N=NH and Fe–N(H^+) bond lengths corresponding to different electronic states (q, M_s) of $[(CpIr)_3(FeN{=}NH)(\mu_3\text{-}S)_4]^{+q}$ computed at the B3LYP/LACVP+* level of theory.

only noticeable elongation was observed when the charge of the cluster was negative.

The sabbatical stay of P.M.K. at Kyushu University was supported by the Institute for Materials Chemistry and Engineering. K.Y. acknowledges Grants-in-Aid (Nos. 18350088, 18GS02070005, and 18066013) for Scientific Research from Japan Society for the Promotion of Science (JSPS) and the Ministry of Education, Culture, Sports, Science and Technology of Japan (MEXT), the Nanotechnology Support Project of MEXT, the Joint Project of Chemical Synthesis Core Research Institutions of MEXT, and CREST of Japan Science and Technology Agency for their support of this work. Financial support by CREST of JST and by Grant-in-Aid for Scientific Research on Priority Areas (No. 14078206, "Reaction Control of Dynamic Complexes") from the Ministry of Education, Culture, Sports, Science and Technology, Japan, to Y.M. is also appreciated.

Supporting Information

Four Tables of the Cartesian coordinates for optimized structures of the $[(CpIr)_3(FeN_2)(\mu_3\text{-}S)_4]$ cluster and the detailed crystallographic data for **1**. This material is available free of charge on web at http://www.csj.jp/journals/bcsj/.

References

1 a) B. E. Smith, *Adv. Inorg. Chem.* **1999**, *47*, 160. b) J. B. Howard, D. C. Rees, *Chem. Rev.* **1996**, *96*, 2965. c) B. K. Burgess, D. J. Lowe, *Chem. Rev.* **1996**, *96*, 2983. d) R. R. Eady, *Chem. Rev.* **1996**, *96*, 3013. e) B. E. Smith, M. C. Durrant, S. A. Tairhurst, C. A. Gormal, K. L. C. Grönberg, R. A. Henderson, S. K. Ibrahim, T. LeGall, C. J. Pickett, *Coord. Chem. Rev.* **1999**, *185–186*, 669.

2 a) R. Schlögl, *Angew. Chem., Int. Ed.* **2003**, *42*, 2004. b) G. J. Leigh, in *Catalysts for Nitrogen Fixation*, ed. by B. E. Smith, R. L. Richards, W. E. Newton, Kluwer, Dordrecht, **2004**, pp. 33–54.

3 O. Einsle, F. A. Tezcan, S. L. A. Andrade, B. Schmid, M. Yoshida, J. B. Howard, D. C. Rees, *Science* **2002**, *297*, 1696.

4 a) I. Dance, *Chem. Commun.* **2003**, 324. b) B. Hinnemann, J. K. Norskov, *J. Am. Chem. Soc.* **2003**, *125*, 1466. c) T. Lovell, T. Liu, D. A. Case, L. Noodleman, *J. Am. Chem. Soc.* **2003**, *125*, 8377. d) U. Huniar, R. Ahlrichs, D. Coucouvanis, *J. Am. Chem. Soc.* **2004**, *126*, 2588.

5 a) M. Hidai, Y. Mizobe, *Can. J. Chem.* **2005**, *83*, 358. b) Barriere, *Coord. Chem. Rev.* **2003**, *236*, 71. c) P. L. Holland, in *Comprehensive Coordination Chemistry II*, ed. by J. McCleverty, T. J. Meyer, Elsevier, Oxford, **2003**, pp. 569–599. d) B. A. Mackay, M. D. Fryzuk, *Chem. Rev.* **2004**, *104*, 385. e) D. Sellmann, J. Utz, N. Blum, F. W. Heinemann, *Coord. Chem. Rev.* **1999**, *190–192*, 607. f) M. Hidai, Y. Mizobe, *Chem. Rev.* **1995**, *95*, 1115. g) R. L. Richards, *Coord. Chem. Rev.* **1996**, *154*, 83. h) G. J. Leigh, *Acc. Chem. Res.* **1992**, *25*, 177.

6 a) M. Hidai, Y. Mizobe, in *Molybdenum and Tungsten: Their Roles in Biological Processes*, ed. by A. Sigel, H. Sigel, Marcel Dekker, New York, **2002**, pp. 121–161. b) D. V. Yandulov, R. R. Schrock, *Science* **2003**, *301*, 76. c) V. Ritleng, D. V. Yandulov, W. W. Weare, R. R. Schrock, A. S. Hock, W. M. Davis, *J. Am. Chem. Soc.* **2004**, *126*, 6150. d) R. L. Richards, *Coord. Chem. Rev.* **1996**, *154*, 83. e) J. Chatt, J. R. Dilworth, R. L. Richards, *Chem. Rev.* **1978**, *78*, 589.

7 a) P. C. Dos Santos, R. Y. Igarashi, H.-I. Lee, B. M. Hoffman, L. C. Seefeldt, D. R. Dean, *Acc. Chem. Res.* **2005**, *38*, 208. b) P. L. Holland, *Can. J. Chem.* **2005**, *83*, 296. c) R. Y. Igarashi, M. Laryukhin, P. C. Dos Santos, H.-I. Lee, D. R. Dean, L. C. Seefeldt, B. M. Hoffmann, *J. Am. Chem. Soc.* **2005**, *127*, 6231. d) B. M. Barney, R. Y. Igarashi, P. C. Dos Santos, D. R. Dean, L. C. Seefeldt, *J. Biol. Chem.* **2004**, *279*, 53621. e) H.-I. Lee, R. Y. Igarashi, M. Laryukhin, P. E. Doan, P. C. Dos Santos, D. R. Dean, L. C. Seefeldt, B. M. Hoffman, *J. Am. Chem. Soc.* **2004**, *126*, 9563. f) B. M. Barney, H.-I. Lee, P. C. Dos Santos, B. M. Hoffman, D. R. Dean, L. C. Seefeldt, *Dalton Trans.* **2006**, 2277. g) J. Kästner, P. E. Blöchl, *J. Am. Chem. Soc.* **2007**, *129*, 2998. h) I. Dance, *J. Am. Chem. Soc.* **2007**, *129*, 1076.

8 For recent examples of $Fe\text{–}N_2$ complexes, see: a) T. A. Betley, J. C. Peters, *J. Am. Chem. Soc.* **2003**, *125*, 10782. b) T. A. Betley, J. C. Peters, *J. Am. Chem. Soc.* **2004**, *126*, 6252. c) C. E. MacBeth, S. B. Hawkins, J. C. Peters, *Can. J. Chem.* **2005**, *83*, 332. d) S. C. Bart, E. Lobkovsky, P. J. Chirik, *J. Am. Chem. Soc.* **2004**, *126*, 13794. e) J. M. Smith, R. J. Lachicotte, K. A. Pittard, T. R. Cundari, G. Lukat-Rodgers, K. R. Rodgers, P. L. Holland, *J. Am. Chem. Soc.* **2001**, *123*, 9222. f) J. Vela, S. Stoian, C. J. Flaschenriem, E. Münck, P. L. Holland, *J. Am. Chem. Soc.* **2004**, *126*, 4522. g) J. M. Smith, A. R. Sadique, T. R. Cundari, K. R. Rodgers, G. Lukat-Rodgers, R. J. Lachicotte, C. J. Flaschenriem, J. Vela, P. L. Holland, *J. Am. Chem. Soc.* **2006**, *128*, 756.

9 a) J. D. Gilbertson, N. K. Szymczak, D. R. Tyler, *J. Am. Chem. Soc.* **2005**, *127*, 10184. b) A. Hills, D. L. Hughes, M. Jimenez-Tenorio, G. J. Leigh, A. T. Rowley, *J. Chem. Soc., Dalton Trans.* **1993**, 3041.

10 Quite recently, we have succeeded in a isolation of the cubane-type cluster having the N_2 ligand, $[(Cp^*Ir)_3\{Ru(N_2)(TMEDA)\}(\mu_3\text{-}S)_4]$ (TMEDA = $Me_2NCH_2CH_2NMe_2$). To the best of our knowledge, this is the first example of the N_2-ligating metal sulfido clusters, but in this cluster, the N_2 molecule is bonded to the octahedral Ru center: H. Mori, H. Seino, M. Hidai, Y. Mizobe, *Angew. Chem., Int. Ed.* **2007**, *46*, 5431.

11 K. Yoshizawa, N. Kihara, Y. Shiota, H. Seino, Y. Mizobe, *Bull. Chem. Soc. Jpn.* **2006**, *79*, 53.

12 *CrystalStructure 3.00: Crystal Structure Analysis Package*, Rigaku and Rigaku/MSC, **2000–2002**; D. J. Watkin, C. K. Prout, J. R. Carruthers, P. W. Betteridge, *CRYSTALS Issue 10*, Chemical Crystallography Laboratory, Oxford, UK.

13 P. T. Beurskens, G. Admiraal, G. Beurskens, W. P. Bosman, S. Garcia-Granda, R. O. Gould, J. M. M. Smits, C. Smykall, *PATTY: The DIRDIF Program System*, Technical Report of the Crystallography Laboratory, University of Nijmegen, Nijmegen, The Netherlands, **1992**.

14 P. T. Beurskens, G. Admiraal, G. Beurskens, W. P. Bosman, R. de Gelder, R. Israel, J. M. M. Smits, *DIRDIF99: The DIRDIF-99 Program System, Technical Report of the Crystallography Laboratory*, University of Nijmegen, Nijmegen, The Netherlands, **1999**.

15 a) A. D. Becke, *Phys. Rev. A* **1988**, *38*, 3098. b) A. D. Becke, *J. Chem. Phys.* **1993**, *98*, 5648.

16 C. Lee, W. Yang, R. G. Parr, *Phys. Rev. B* **1988**, *37*, 785.

17 *Jaguar 5.0*, Schrödinger, LLC, Portland, Oregon, **2002**.

18 R. A. Torres, T. Lovell, L. Noodleman, D. A. Case, *J. Am. Chem. Soc.* **2003**, *125*, 1923.

19 a) Y. Mizobe, in *Handbook of Chalcogen Chemistry*, ed. by F. A. Devillanova, Royal Society of Chemistry, **2006**, pp. 725–741. b) U. Huniar, R. Ahlrichs, D. Coucouvanis, *J. Am. Chem. Soc.* **2004**, *126*, 2588.

20 R. R. Schrock, *Acc. Chem. Res.* **2005**, *38*, 955.

21 F. Studt, F. Tuczek, *J. Comput. Chem.* **2006**, *27*, 1278.

22 F. Neese, *Angew. Chem., Int. Ed.* **2006**, *45*, 196.